Evaluation of the intensity measure approach in PBEE through the use of simulated ground motions

A. Quiroz-Ramírez
Universidad Nacional Autónoma de México, México.

D. Arroyo & A. Terán-Gilmore
Universidad Autónoma Metropolitana, México.

M. Ordaz
Universidad Nacional Autónoma de México, México.

SUMMARY:
The incremental dynamic analysis has become a popular option to statistically characterize the seismic demands on systems undergoing significant plastic behavior. In spite of its extensive use within performance-based earthquake engineering, there are still issues that haven't been sufficiently understood, such as the use of this type of analysis for structures located at very soft soil sites, and the use of duration dependent engineering demand parameters. Also, there is a need to study the implications in terms of the accuracy implicit in the use of its results to carry out a hazard analysis. To help clarify these issues, the dynamic response of single-degree-of-freedom systems is studied under the consideration of different types of ground motions. The discussion offered herein provides a general understanding of the applicability of an incremental dynamic analysis, and help identify situations in which a more sophisticated analysis may be warranted.

Keywords: Incremental dynamic analysis, performance-based earthquake engineering, Seismic hazard

1. INTRODUCTION

Thanks to the research carried by Vamvatsikos and Cornell (2002) and Fragiadakis and Vamvatsikos (2010), among others, the *Incremental Dynamic Analysis* (*IDA*) has become the state-of-the-art approach to statistically characterize the inelastic seismic demands within the context of *Performance-Based Earthquake Engineering* (*PBEE*). Complementary research has studied the use of the *Intensity Measure* (*IM*) approach within PBEE, and other studies have dealt with the issue of ground motion scaling (Iervolino and Cornell 2005, Baker and Cornell 2005, Tothong and Cornell 2006, Luco and Cornell 2007).

Vamvatsikos and Cornell (2002) discussed the fundamentals of the *IDA* and provided a unifying conceptual basis. Based on the study of the dynamic response of single and multi-degree-of-freedom (SDOF and MDOF, respectively) systems subjected to ground motion records corresponding to NEHRP C-D soil classes, Iervolino and Cornell (2005) concluded that there should be no concern when selecting records to match a specific magnitude-distance scenario. Nevertheless, they acknowledged that the characteristics of the records that were used in their studies (with magnitude, M_w, ranging from 6.4 to 7.4) may condition this observation.

In terms of ground motion scaling, Baker and Cornell (2005) proposed a vector-valued ground motion intensity measure, and demonstrated that a vectorial characterization of the elastic spectral acceleration corresponding to the fundamental period of vibration, $S_A(T_1)$, merged into a significantly superior intensity measure. This kind of intensity measure included the definition of parameter ε, which corresponds to the number of standard deviations by which an observed logarithmic spectral acceleration differs from the mean logarithmic spectral acceleration computed from a ground motion prediction equation.

Although the use of the *IDA* to predict seismic demands has been extensively studied, some issues still need understanding. This paper focuses its attention on three of these issues. Firstly, while the use of

Engineering Demand Parameters (*EDP*) related to peak displacement (e.g., ductility and inter-story drift index) has been thoroughly studied; other seismic demands that may be relevant to seismic performance haven't been adequately studied (Shome et al. 1998). In order to limit the discussion presented herein, only two *EDP*s will be considered: A) Peak ductility (μ), which can be considered fairly independent of ground motion duration; and B) Normalized plastic energy ($NE_{H\mu}$) which may strongly depend on duration. $NE_{H\mu}$ is defined as the energy contained in all the hysteretic loops a system undergoes during the ground motion normalized by the product of the strength and displacement at first yield.

A second issue that deserves attention has to do with the fact that results obtained so far are usually conditioned by the set of ground motions that have been used, particularly because of the lack of records in some magnitude-distance bins (e.g., large-magnitude events). In an attempt to overcome this limitation, the studies presented herein use synthetic ground motions established through a stochastic simulation method that is consistent with seismological theory. Within this context, ground motions exhibiting narrow and wide-banded frequency contents are considered. It should be mentioned that Tothong and Cornell (2006) used a similar approach to the one described herein, and observed some differences between the *IDA*'s results and those corresponding to the use of simulated records. It is important to consider that these researchers used a point-source model to simulate ground motion records for a 6.8 M_w event and epicentral distances of 18 km, scenario in which the source model could not represent accurately the existing near-source effects (particularly, the saturation with magnitude of the spectral acceleration at high frequencies).

A third issue that deserves attention is that available studies claim that if the regression of *EDP* jointly on *IM* is found to be effectively independent of M_w and the closest distance to the rupture area (*RCLD*), the median *IDA* curve leads to accurate estimates of *EDP* related to a certain rate of exceedance (Vamvatsikos and Cornell 2002, Luco and Cornell 2007). In an attempt to provide some context in terms of how accurate these estimates can be; this paper compares analytically derived hazard curves with empirical curves established from a set of synthetic ground motions that are representative of a given hazard environment.

2. SITES AND GROUND MOTION SETS

The studies described herein considered ground motions recorded during seven inter-plate seismic events that occurred along the Mexican subduction zone.

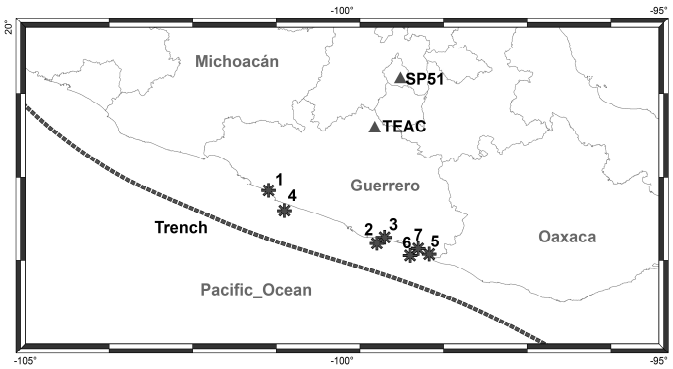

Figure 1. Events and sites considered in the analysis

While Figure 1 locates the epicenters of the events, Table 1 summarizes their characteristics. While M_0 denotes seismic moment; H is the focal depth; and $\Delta\sigma$, the stress parameter. While M_w, M_0, H and the epicenters of the seismic events were established according to Pacheco and Singh (2010), the stress parameter for the first four events was defined according to Humphrey and Anderson (1994); and

according to Singh et al. (2000), Ordaz and Singh (1992), and Kohrs-Sansorny et al. (2005), respectively, for the fifth, sixth and seventh events. Note from Table 1 that the ground motions under consideration were recorded during small and moderate seismic events.

The sites under consideration are also located in Figure 1. While TEAC is located at a firm soil site in the State of Guerrero with soil conditions that are consistent with those of NEHRP B soil class; SP51 is located at the lake-bed zone of Mexico City, comprised by 10 to 100 m deep deposits of highly compressive and high water content clay underlain by resistant sands (Ordaz and Singh 1992). Both sites are located roughly at 200 and 300 *km* from the seismic sources. The Mexico City motions exhibit narrow-banded frequency content and a very high spectral amplification around the dominant frequency of motion (which can range from 0.2 to 0.7 Hz). Under the consideration that two components were recorded at each site during each seismic event, fourteen real accelerograms were available for each site.

Table 1. Seismic events used in the analysis

Event	Date	M_w	M_0 (dyna-cm)	$\Delta\sigma$ [bar]	H [km]	Source
1	08/02/1988	5.8	7.37E+24	524	22	Petatlán
2	25/04/1989	6.9	2.39E+26	89	16	San Marcos
3	02/05/1989	5.5	1.91E+24	154	15	San Marcos
4	31/05/1990	5.9	7.49E+24	145	18	Guerrero Central
5	15/05/1993	5.5	1.41E+25	129	16	Ometepec
6	24/10/1993	6.6	1.01E+26	10	26	Ometepec
7	14/09/1995	7.3	1.31E+27	10	16	Ometepec

To achieve the objectives of this paper, three sets of ground motions were conformed for each site. The first set, denoted *SET1*, is comprised for each site by the fourteen recorded motions. Because of the lack of recorded motions during events with M_w of 7.0 or larger, the linear scaling factors required by the motions of *SET1* to obtain meaningful *IDA* curves are significantly larger than those used in previous studies. Particularly, while the peak scaling factors under consideration herein are of the order of one hundred, Iervolino and Cornell (2005) used peak factors close to six. In terms of magnitude, this implied scaling up the motions three and one units of magnitude, respectively.

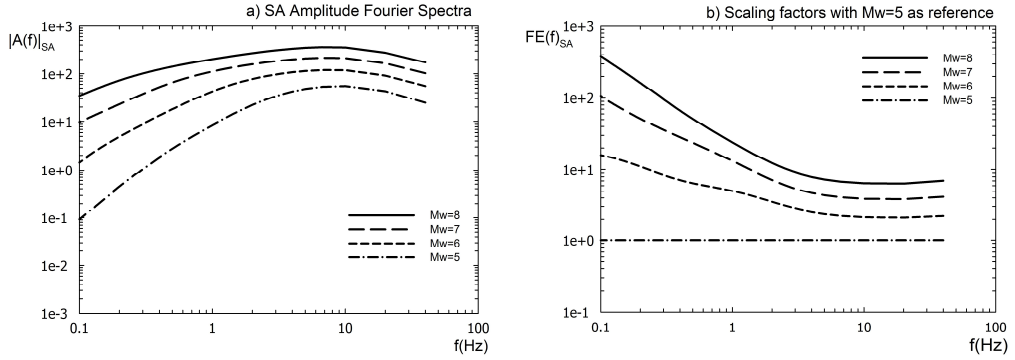

Figure 2. a) Fourier pseudo-acceleration amplitude spectra for values of M_w in the range between 5 and 8; b) Scaling factors using M_w of 5 as reference

The influence of M_w and *RCLD* on the scaling of ground motion records has been thoroughly studied within the seismological field, and several scaling methods consistent with the seismological theory have been developed (Boore 1983, Irikura and Kamae 1994, Joyner and Boore 1986, Somerville et al. 1991, Kanamori et al. 1993, Ordaz et al. 1995, Kohrs-Sansorny et al. 2005). Available methods include the use of theoretical and empirical Green's functions, stochastic finite-fault models, stochastic point-source models and the finite differences technique. Figure 2a compares Fourier Amplitude Spectra corresponding to pseudo-acceleration and different values of M_w (Atkinson and Silva 2000). The change in the shape of the Fourier spectra with increasing magnitude is evident, particularly for

frequencies smaller than 3 Hz. Figure 2b shows the factors required to scale the spectral ordinates corresponding to the Fourier spectrum for M_w of 5 up to the spectral values corresponding to other values of M_w. Note the strong dependence that the scaling factors exhibit with respect to frequency, and the fact that the linear scaling method under consideration in the *IDA* disregards these dependence.

For the second set of records (denoted herein as *SBSET*), it was decided to use the Kohrs-Sansorny et al. (2005) two-stage summation simulation technique to generate synthetic ground motions. The technique requires two parameters for the target event: M_0 and $\Delta\sigma$. Ground motions were simulated for different postulated values of M_w considering magnitude intervals of 0.1. For the first, fourth and fifth events, ground motion records were generated for M_w ranging from 6.5 to 8.2. The magnitudes under consideration for the second, third, sixth and seventh events are: A) 7.5 to 8.2; B) 6.0 to 8.2; C) 7.0 to 8.2; and D) 8.0 to 8.2; respectively. For each postulated value of M_w, ten synthetic ground motions were generated for each available empirical Green's function, yielding a total of 2020 records.

Figure 3 compares S_A spectra obtained from the synthetic and actual ground motions. The comparison considers for each site the 12.5, 50.0 and 87.5 percentiles of all simulated records for M_w of 8.0 (dashed lines). In addition, the figure includes the S_A spectra corresponding to the geometric mean of the two horizontal components recorded at the sites under consideration in this paper during the 1985 Michoacan earthquake. Note that the properties of the synthetic records are consistent with those of the actual ground motions in spite of the fact that ground motions for the Michoacan region were not used as Green's functions.

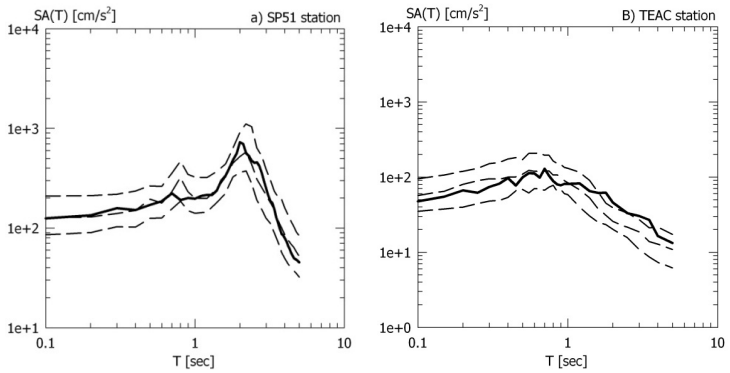

Figure 3. Comparison of S_A spectra derived from simulated and actual ground motions for an event with M_w of 8.

Finally and to fully achieve the objectives of this paper, a third set of ground motions, denoted *SET2*, was formed with 100 synthetic ground motions established for M_w of 7.0 by using five of the fourteen records that comprise *SET1* as Green functions within the Kohrs-Sansorny et al. methodology. Because of the larger magnitude they are associated with in relation with the motions included in *SET1*, the motions in *SET2* require much smaller scaling factors (ranging from 0.1 to 10.0) to cover the full range of magnitudes under consideration to obtain the *IDA* curves. Within this context, the motions need to be scaled up and down one unit of magnitude. In this sense and in terms of linear scaling, the *SET2* motions conform to the type of motions used so far on *IDA* studies.

3. SINGLE-DEGREE-OF-FREEDOM SYSTEMS

An *Elasto-Perfectly Plastic* (*EPP*) hysteretic model was considered for the studies reported herein. This model is defined by the system's period (T) and its yield strength, characterized through the seismic coefficient c, which in turn is defined as the yield strength normalized by the system's weight. Although simple, this hysteretic model is able to provide reasonable seismic demand predictions for a broad range of nonlinear structures (Tothong and Cornell 2006, Tothong and Luco 2007).

The single-degree-of-freedom (*SDOF*) systems under consideration herein have *T* of 2.0 seconds and *c* of 0.1 for the *SP51* site, and *T* of 0.8 seconds and *c* of 0.05 for the *TEAC* site. Quiroz (2012) reports the results corresponding to *SDOF* systems with a wide variety of structural properties and other type of hysteretic behavior.

4. PROCEDURE

Two standard multi-record *IDA* analyses were performed to establish median *IDA* curves for the *EDP*s under consideration: one for *SET1*, and a second for *SET2*. The *IDA*s carried out with the ground motions included in *SET1* and *SET2* are denoted, respectively, *IDASET1* and *IDASET2*. Then, a third series of dynamic analyses were carried out by using the *SBSET*. Although the results derived from the motions included in *SBSET* can be plotted in a standard *IDA* curve format, this type of analysis cannot be considered an *IDA*. The dynamic analyses that use the *SBSET* will be referred herein as seismological-based dynamic analysis (*SBDA*).

To better achieve the objectives of this work, the median curves derived from the dynamic analyses considered the normalization of its ordinates by the system's strength. In this manner, the evolution of the *EDP* can be observed as a function of an increase in *R*, where *R* is a strength reduction factor defined as the ratio of the pseudo acceleration ordinate corresponding to the period of the *SDOF* system, $S_A(T_1)$, and its seismic coefficient. Within this context, the results derived from the *SBDA* can be compared with those corresponding to the *IDASET1* and *IDASET2*, and the accuracy of the *IDA* can be quantified through the statistics of parameter *z*, defined as:

$$z(EDP_i) = \ln(EDP_i) - \ln\left(EDP_i^{IDA}\right) \tag{1}$$

where EDP_i is, within the context of a *SBDA*, the *EDP* corresponding to the *ith* value of the *IM*; and EDP_i^{IDA} is the ordinate of the *IDA* median curve corresponding to the same value of *IM*. Let *b* denote the expected value and of *z*. Note that the former parameter is a measure of the bias introduced by linearly scaling the ground motions within the context of an *IDA*. While a positive value of *b* implies that the median *IDA* curve, on average, underestimates the results of the *SBDA*; a negative value implies an overestimation.

For the second part of the analysis, S_A is considered as the *IM*. The median *IDA* curve and its logarithm related standard deviation were used to estimate rates of exceedance according to:

$$\nu(EDP) = \int_0^\infty P(EDP > edp | IM) \left| \frac{d\nu(IM)}{dIM} \right| dIM \tag{2}$$

where $\nu(IM)$ represents the hazard curve for the *IM*, and $P(EDP>edp|\ IM)$ is the probability of *EDP* exceeding the value of *edp*, conditioned on *IM* and on the properties of the *SDOF* system. In order to compute $P(EDP>edp|\ IM)$, it is assumed that the conditional probability density function of *EDP* given *IM* follows a lognormal probability density function whose parameters are obtained from the *IDA*.

5. RESULTS OF DYNAMIC ANALYSES

Figures 5 and 7 summarize the *IDA* curves for the two *SDOF* models under consideration (one located at *SP51*, and the other one at *TEAC*). While the black lines correspond to the *SBDA*, the continuous and dashed grey lines refer to the *IDASET1* and *IDASET2*, respectively. While values of *R* less than 1.0 correspond to elastic response, values larger than 1.0 imply non-linear behaviour. Within this context, it can be said that if the *EDP*s corresponding to the different types of dynamic analysis are

similar for values of *R* larger than one, the linear scaling implied by the use of an *IDA* is capable of offering a reasonable characterization of the nonlinear demands in the *SDOF* systems.

Figure 5 shows, for the *SP51* site, significant differences between the *SBDA* demands and those implied by both median *IDA* curves. The differences tend to increase with an increase in *R*, and the median *IDA* curves tend to overestimate the *EDP* demands. In terms of ductility (Figure 5a), the differences between the *IDAs* and the *SBDA* are quantified at 5% for *R* of 5.5, 10% for *R* of 6.3, and 20% for *R* of 11.1. In the case of $NE_{H\mu}$, these percentages correspond to *R* values of 1.5, 2.5 and 12.4, respectively. Note that the residuals (values of *b*) shown in Figure 6 support the notion that the *IDA* tends to overestimate the nonlinear seismic demands on the *SDOF* system.

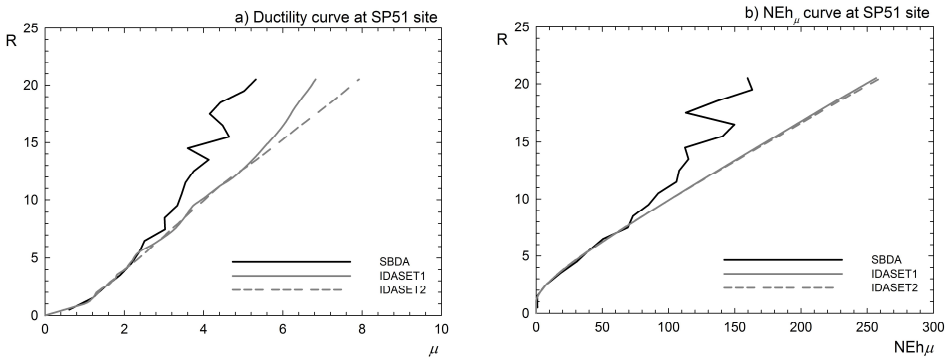

Figure 5. Median curves derived from the different dynamic analyses, *SP51* site

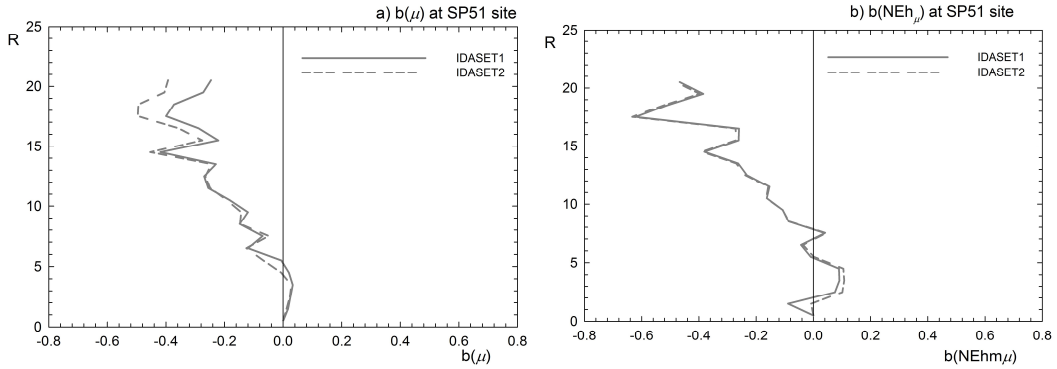

Figure 6. Residuals corresponding to *IDASET1* and *IDASET2*, *SP51* site

In the case of the *TEAC* site (firm soil), Figure 7 shows that, even if the bias follows a similar tendency than that discussed for *SP51*, significant differences can be observed for *R* slightly larger than one. In the case of ductility, the average differences between both *IDA* analysis and the *SBDA* can be quantified at 5% for *R* of 1.1, 10% for *R* of 1.2, and 20% for *R* of 1.5. In the case of $NE_{H\mu}$, the *R* values are 2.2, 2.9 and 4.2, respectively. Note that Figure 8 makes evident that for the firm soil case, the bias associated to the *IDA*s becomes important at very low values of *R*.

6. PERFORMANCE-BASED EARTHQUAKE ENGINEERING COMPUTATIONS

This section considers the *SP51* and *TEAC* sites and four seismic sources: Petatlán, Guerrero Central, San Marcos and Ometepec (events 1, 4, 2 and 5, respectively, in Table 1 and Figure 1). For simplicity sake and taking into consideration that the epicentral distances are larger than 100 km, the seismic sources were modelled as a single-point-source.

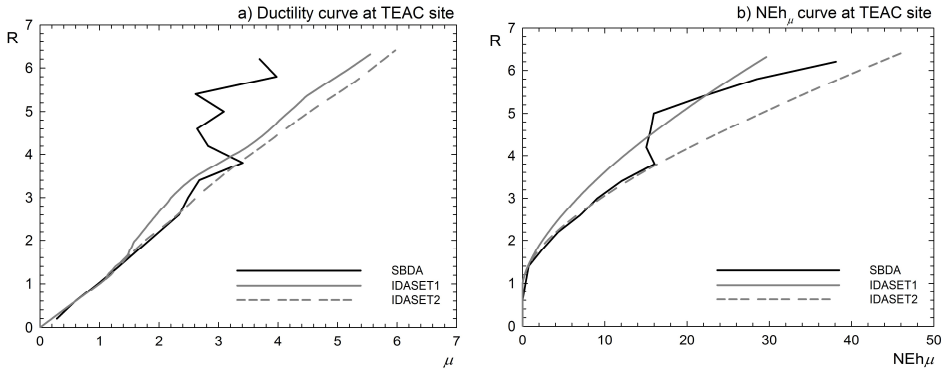

Figure 7. Median curves derived from the different dynamic analyses, *TEAC* site

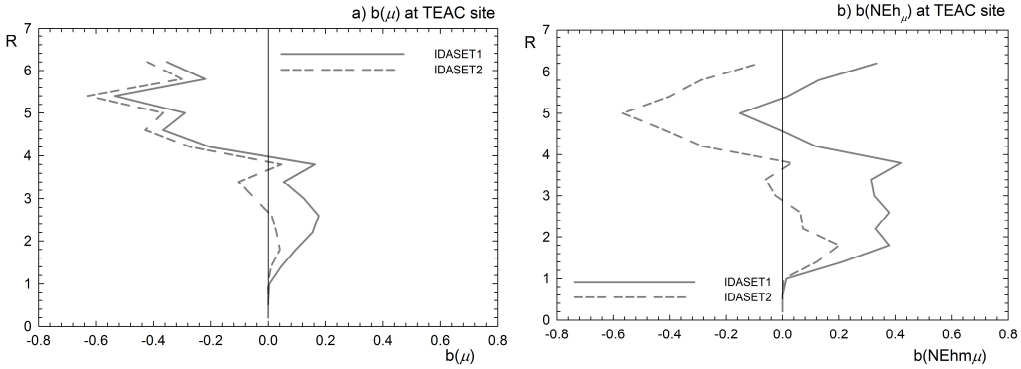

Figure 8. Residuals corresponding to *IDASET1* and *IDASET2*, *TEAC* site

Figure 9 shows empirical hazard curves for S_A. The figure contemplates the total hazard curve and a hazard curve for each source. In practice, only the total hazard curve would be available. For *SP51*, the San Marcos source controls the total hazard curve for rates of exceedance smaller than 0.005/year. At *TEAC*, the total hazard curve has a more uniform influence of every source. With the total S_A hazard curves, and the median *IDA* curve for a given *EDP* and its logarithmic standard deviation, it is possible to establish analytical hazard curves for that *EDP* by using Equation 2.

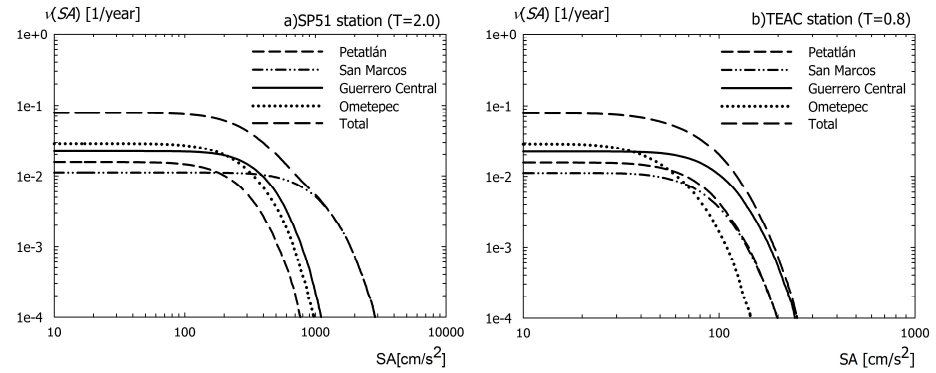

Figure 9. S_A hazard curves corresponding to the *SP51* and *TEAC* sites

Figure 10 shows that for the *SDOF* located at *SP51*, significant differences can be observed in the hazard curves derived from the different dynamic analyses for μ and $NE_{H\mu}$. For ν(*EPD*) smaller than 0.05 and 0.01, respectively, the analytical hazard curves derived from the *IDASET1* and *IDASET2* result in larger seismic demands than those corresponding to the empirical hazard curves. In the case

of μ, the *IDASET1* yields differences of about 28%, 59% and 82% for ν of 0.01, 0.001 and 0.0001/year, respectively; and the *IDASET2* differences of 48%, 108% and 182%, respectively. In the case of $NE_{H\mu}$, the differences are 15%, 60% and 80%, respectively, for the *IDASET1*; and 15%, 67% and 95%, respectively, for the *IDASET2*. Within this context, it is important to understand that a median *IDA* curve is not only biased with respect to M_w or *RCLD*, but also with respect to the seismic sources (due to differences on path, azimuth and characteristics at the source).

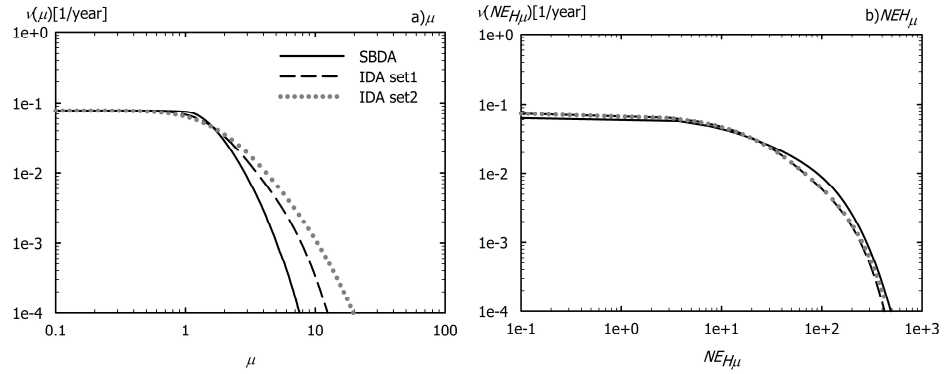

Figure 10. Comparison of μ and $E_{H\mu}$ hazard curves for *SDOF* located at the *SP51* site

For the *SDOF* system located at *TEAC*, Figure 11 shows smaller differences than those observed in Figure 10. In the case of μ, the *IDASET1* yields differences of 5%, 11% and 0.1% for ν values of 0.01, 0.001 and 0.0001/year, respectively. Differences of 23%, 42% and 32%, respectively, are observed for the *IDASET2*. In the case of $NE_{H\mu}$, differences of 28%, 37% and 45%, respectively, are observed for the *IDASET1*; and of 7%, 15% and 26%, respectively, for the *IDASET2*.

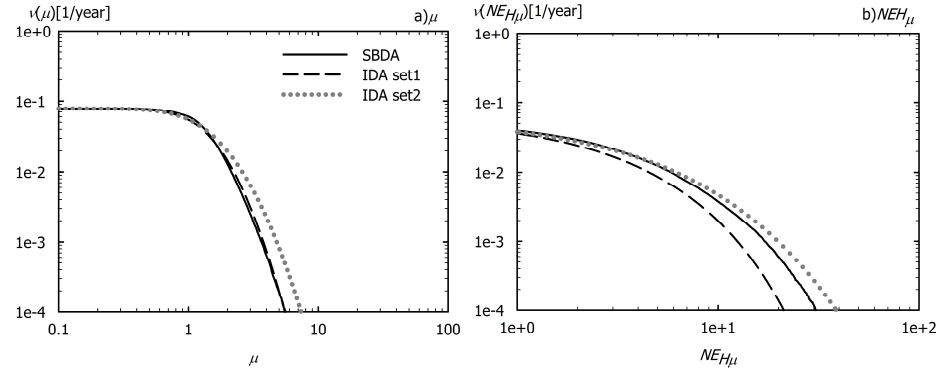

Figure 11. Comparison of μ and $E_{H\mu}$ hazard curves for *SDOF* located at the *TEAC* site

7. DISCUSSION AND CONCLUSIONS

Although the results presented herein are limited to the: A) Ground motion records used as empirical Green's functions; B) Number of seismic sources and their locations; C) Ratio between the stress parameters of the target event and those of the empirical Green's function; and D) Hysteretic behaviour under consideration; it can be said that they have important implications within the framework of *PBEE*.

An *IDA* may introduce bias with respect to the seismic sources. For simplicity sake, in the examples presented herein four seismic point-sources, practically equidistant to the sites under consideration, were considered. Within this context, the effect of bias with respect to the seismic sources may have been magnified.

On one hand, it may be concluded that linear scaling of motions without any physical constraint may result in the scaling up of some records to physically impossible values of *IM*, which in turn may result in inaccurate estimates of the *EDP*. On the other hand, it should be considered that seismological theory establishes consistent physical constraints for the scaling of ground motion records.

It is a fact that a joint regression of *EDP* on *IM*, conditioned to be independent of M_w and *RCLD*, does not necessarily lead to accurate estimates of *EDP* within *PBEE*; particularly when certain seismic sources systematically generate ground motions with intensities that are much larger than those expected on the other ones. The *SBDA* could be very helpful in identifying these situations, and in providing information to insure better *EDP* estimations. The *IDA* is a useful technique to estimate seismic demands within the context of *PBEE* and this paper is not an attempt to refute its importance. In fact, the results presented herein may improve the use of the *IDA* within *PBEE*, and may help identify under which circumstances a more refined analysis may be warranted.

AKCNOWLEDGEMENT

The doctoral studies of the first author were supported by the *Consejo Nacional de Ciencia y Tecnología* and the Seismological Engineering and Seismic Instrumentation Coordination from Instituto de Ingeniería. Also, the first author expresses his gratitude to the *Instituto Superior Tecnico* from *Universidad Técnica de Lisboa* for the use of its installations during his doctoral stay.

REFERENCES

Atkinson, G. M., and W. J. Silva (2000). Stochastic modeling of California ground motions. *Bulletin of the Seismological Society of. America* **90:2**,255–274.

Baker, J. W. and Cornell, C. A., (2005). A vector-valued ground motion intensity measure consisting of spectral acceleration and epsilon. *Earthquake Engineering Structural Dynamics* **34**,1193-1217.

Boore, D. M. (1983). Stochastic simulation of high-frequency ground motions based on seismological models of the radiated spectra. *Bulletin of the Seismological Society of. America* **73:6**,1865–1894.

Fragiadakis, M. and Vamvatsikos D. (2010). Fast performance uncertainty estimation via pushover and approximate IDA. *Earthquake Engineering and Structural Dynamics* **39:6,**683–703.

Humprey, J.R. and Anderson J.G., (1994). Seismic source parameters from the Guerrero Subduction Zone. *Bulletin of the Seismological Society of America* **84:6**,1754–1769.

Iervolino, I. and Cornell, C.A. (2005). Record selection for nonlinear seismic analysis of structures. *Earthquake Spectra* **21:3**,685–713.

Irikura, K. and Kamae, K. (1994). Estimation of strong ground motion in broad-frequency band based on a seismic source scaling model and an empirical Green's function technique. *Annals of Geophisycs* **37**,1721-1743.

Joyner, W. B. and D. M. Boore (1986). On simulation large earthquakes by Green's functions addition of smaller earthquakes, in Earthquake Source Mechanics. *American Geophysical Monograph* **37**,269-274.

Kanamori, H., P. C. Jennings, S. K. Singh, and L. Astiz (1993). Estimation of strong ground motions in Mexico City expected for large earthquakes in the Guerrero seismic gap, *Bulletin of the Seismological Society of America* **83**,811-829.

Kohrs–Sansorny C., Courboulex, F., Bour, M. and Deschamps A., (2005). A two – stage method for ground simulation using stochastic summation of small earthquakes. *Bulletin of the Seismological Society of America* **95:4**,1387–1400.

Luco, N. and Cornell, C.A. (2007). Structure-Specific Scalar Intensity Measures for Near-Source and Ordinary Earthquake Ground Motions. *Earthquake Spectra* **23:2**,357-392.

Ordaz, M. and Singh S.K., (1992). Source spectra and spectral attenuation of seismic waves from Mexican earthquakes, and evidence of amplification in the hill zone of Mexico City. *Bulletin of the Seismological Society of America* **82:1**,24–43.

Ordaz, M. Arboleda, J. and Singh S.K., (1995). A scheme of random summation for an empirical Green´s function to estimate ground motions from future large earthquakes. *Bulletin of the Seismological Society of America* **85:6**,1635–1647.

Pacheco, J.F. and Singh S.K., (2010). Seismicity and state of stress in Guerrero segment of the Mexican subduction zone. *Journal of Geophysical Research* **115**,1303–1327.

Quiroz, A., (2012). Un enfoque sismológico del Análisis Dinámico Incremental: Repercusiones sobre el peligro sísmico. *Doctoral thesis, Postgraduate studies program*, UNAM, México.

Shome, N., Cornell, C.A., Bazurro, P., Carballo, J.E. (1998). Earthquakes, Records , and Nonlinear Responses. *Earthquake Spectra* **14:3**,469-500.

Singh, S.K., Pacheco, J., Ordaz, M. and Kostoglodov, V. (2000). Source Time Function and Duration of Mexican Earthquakes. *Bulletin of the Seismological Society of America* **90(2)**,468–482.

Somerville, P, Sen, M. and Cohee, B. (1991). Simulations of strong ground motions recorded during the 1985 Michoacan, México and Valparaiso Chile earthquakes. *Bulletin of the Seismological Society of America* **81**,1–27.

Tothong, P. and Luco, N. (2007). Probabilistic seismic demand analysis using advanced ground motion intensity measures. *Earthquake Engineering and Structural Dynamics* **36**,1837-1860.

Tothong, P. and Cornell, C.A (2006). Probabilistic seismic demand analysis using advanced ground motion intensity measures, attenuation relationships and near-fault effects. *Pacific Earthquake Engineering Research Center*. Report PEER 2006/11.

Vamvatsikos, D. and Cornell, C.A., (2002). Incremental Dynamic Analysis. *Earthquake Engineering Structural Dynamics* **31:3**,491-514.